Terahertz pulsed imaging of knee cartilage

Wai-Chi Kan,[1] Win-Sze Lee,[2] Wing-Hoi Cheung,[2] Vincent P. Wallace,[3] and Emma Pickwell-MacPherson[4,*]

[1]*Department of Electronic Engineering, Chinese University of Hong Kong, Hong Kong*
[2]*Department of Orthopaedics & Traumatology, Chinese University of Hong Kong, Hong Kong*
[3]*School of Physics, University of Western Australia, Crawley,6009, Australia*
[4]*Electronic and Computer Engineering Department, Hong Kong University of Science and Technology, Hong Kong*
**eeemma@ust.hk*

Abstract: Osteoarthritis (OA) is a common form of arthritis caused by cartilage degeneration. In this paper, we investigate the potential use of terahertz (THz) pulsed imaging to quantitatively measure the early symptoms of OA in an animal model. THz images of excised rabbit femoral condyles were taken. We observe THz waves reflected off different layers within samples and demonstrate that the optical delay between reflections can give a quantitative measure of the thicknesses of particular tissues within cartilage.

OCIS codes: (110.6795) Terahertz imaging; (120.4825) Optical time domain reflectometry; (000.1430) Biology and medicine.

References and links

1. "Osteoarthritis," (NIH: National Institute of Arthritis and Musculoskeletal and Skin Diseases), *http://www.nlm.nih.gov/medlineplus/osteoarthritis.html*.
2. A. R. Poole, T. Kojima, T. Yasuda, F. Mwale, M. Kobayashi, and S. Laverty, "Composition and structure of articular cartilage: a template for tissue repair," Clin. Orthop. Relat. Res. (391 Suppl), S26–S33 (2001).
3. Arthritis Research UK, http://www.arthritisresearchuk.org/research/data_on_arthritis/data_on_oa/data_on_knee_osteoarthritis.aspx
4. A. D. Woolf, and B. Pfleger, "Burden of major musculoskeletal conditions," Bull. World Health Organ. **81**(9), 646–656 (2003).
5. H. Mankin, H. Dorfman, L. Lippiell, and A. Zarins, "Biochemical and metabolic abnormalities in articular cartilage from osteo-arthritic human hips. 2. correlation of morphology with biochemical and metabolic data," J. Bone and Joint Surgery **53**, 523–537 (1971).
6. J. Rogowska, C. M. Bryant, and M. E. Brezinski, "Cartilage thickness measurements from optical coherence tomography," J. Opt. Soc. Am. A **20**(2), 357–367 (2003).
7. X. D. Li, S. A. Boppart, J. Van Dam, H. Mashimo, M. Mutinga, W. Drexler, M. Klein, C. Pitris, M. L. Krinsky, M. E. Brezinski, and J. G. Fujimoto, "Optical Coherence Tomography: Advanced Technology for the Endoscopic Imaging of Barrett's Esophagus," Endoscopy **32**(12), 921–930 (2000).
8. C. W. Han, C. R. Chu, N. Adachi, A. Usas, F. H. Fu, J. Huard, and Y. Pan, "Analysis of rabbit articular cartilage repair after chondrocyte implantation using optical coherence tomography," Osteoarthritis Cartilage **11**(2), 111–121 (2003).
9. X. D. Li, S. Martin, C. Pitris, R. Ghanta, D. L. Stamper, M. Harman, J. G. Fujimoto, and M. E. Brezinski, "High-resolution optical coherence tomographic imaging of osteoarthritic cartilage during open knee surgery," Arthritis Res. Ther. **7**(2), R318–R323 (2005).
10. Y. Pan, Z. Li, T. Xie, and C. R. Chu, "Hand-held arthroscopic optical coherence tomography for in vivo high-resolution imaging of articular cartilage," J. Biomed. Opt. **8**(4), 648–654 (2003).
11. C. R. Chu, N. J. Izzo, J. J. Irrgang, M. Ferretti, and R. K. Studer, "Clinical diagnosis of potentially treatable early articular cartilage degeneration using optical coherence tomography," J. Biomed. Opt. **12**(5), 051703 (2007).
12. W. Drexler, D. Stamper, C. Jesser, X. Li, C. Pitris, K. Saunders, S. Martin, M. B. Lodge, J. G. Fujimoto, and M. E. Brezinski, "Correlation of collagen organization with polarization sensitive imaging of in vitro cartilage: implications for osteoarthritis," J. Rheumatol. **28**(6), 1311–1318 (2001).
13. T. Xie, Y. Xia, S. Guo, P. Hoover, Z. Chen, and G. M. Peavy, "Topographical variations in the polarization sensitivity of articular cartilage as determined by polarization-sensitive optical coherence tomography and polarized light microscopy," J. Biomed. Opt. **13**(5), 054034 (2008).
14. N. Ugryumova, J. Jacobs, M. Bonesi, and S. J. Matcher, "Novel optical imaging technique to determine the 3-D orientation of collagen fibers in cartilage: variable-incidence angle polarization-sensitive optical coherence tomography," Osteoarthritis Cartilage **17**(1), 33–42 (2009).

#132311 - $15.00 USD Received 26 Jul 2010; revised 16 Sep 2010; accepted 17 Sep 2010; published 20 Sep 2010

15. R. M. Woodward, V. P. Wallace, D. D. Arnone, E. H. Linfield, and M. Pepper, "Terahertz pulsed imaging of skin cancer in the time and frequency domain," J. Biol. Phys. **29**(2/3), 257–259 (2003).
16. A. J. Fitzgerald, V. P. Wallace, M. Jimenez-Linan, L. Bobrow, R. J. Pye, A. D. Purushotham, and D. D. Arnone, "Terahertz pulsed imaging of human breast tumors," Radiology **239**(2), 533–540 (2006).
17. E. Pickwell, V. P. Wallace, B. E. Cole, S. Ali, C. Longbottom, R. J. M. Lynch, and M. Pepper, "A comparison of terahertz pulsed imaging with transmission microradiography for depth measurement of enamel demineralisation in vitro," Caries Res. **41**(1), 49–55 (2007).
18. D. M. Mittleman, R. H. Jacobsen, and M. C. Nuss, "T-ray imaging," IEEE J. Sel. Top. Quantum Electron. **2**(3), 679–692 (1996).
19. M. H. Lu, J. L. Shen, N. Li, Y. Zhang, C. L. Zhang, L. S. Liang, and X. Y. Xu, "Detection and identification of illicit drugs using terahertz imaging," J. Appl. Phys. **100**(10), 103104 (2006).
20. B. M. Fischer, M. Hoffmann, H. Helm, R. Wilk, F. Rutz, T. Kleine-Ostmann, M. Koch, and P. U. Jepsen, "Terahertz time-domain spectroscopy and imaging of artificial RNA," Opt. Express **13**(14), 5205–5215 (2005).
21. J. A. Zeitler, D. A. Newnham, P. F. Taday, T. L. Threlfall, R. W. Lancaster, R. W. Berg, C. J. Strachan, M. Pepper, K. C. Gordon, and T. Rades, "Characterization of temperature-induced phase transitions in five polymorphic forms of sulfathiazole by terahertz pulsed spectroscopy and differential scanning calorimetry," J. Pharm. Sci. **95**(11), 2486–2498 (2006).
22. K. L. Wang, and D. M. Mittleman, "Metal wires for terahertz wave guiding," Nature **432**(7015), 376–379 (2004).
23. S. Atakaramians, S. Afshar V, B. M. Fischer, D. Abbott, and T. M. Monro, "Porous fibers: a novel approach to low loss THz waveguides," Opt. Express **16**(12), 8845–8854 (2008).
24. Y. B. Ji, E. S. Lee, S. H. Kim, J. H. Son, and T. I. Jeon, "A miniaturized fiber-coupled terahertz endoscope system," Opt. Express **17**(19), 17082–17087 (2009).
25. P. Knobloch, C. Schildknecht, T. Kleine-Ostmann, M. Koch, S. Hoffmann, M. Hofmann, E. Rehberg, M. Sperling, K. Donhuijsen, G. Hein, and K. Pierz, "Medical THz imaging: an investigation of histo-pathological samples," Phys. Med. Biol. **47**(21), 3875–3884 (2002).
26. E. Jung, H. Park, J. Kim, Y. Han, H. Han, S. Kim, I. Park, J. Cui, B. Min, and H. Lim, "THz pulse imaging of human articular cartilage," in *Infrared Millimeter Waves and 14th International Conference on Teraherz Electronics 2006, IRMMW-THz 2006, Joint 31st International Conference* (2006), p. 550.
27. E. Pickwell-Macpherson, W. C. Kan, W. S. Lee, V. P. Wallace, and W. H. Cheung, "Application of Terahertz Imaging to Osteoarthritis," *Microwave Symposium Digest 2008, IEEE MTT-S International* (2008), p. 1533–1536.
28. W. C. Kan, W. S. Lee, W. H. Cheung, and E. Pickwell-Macpherson, "A pilot study of terahertz pulsed imaging of osteoarthritis," in *Infrared, Millimeter and Terahertz Waves, 2008. IRMMW-THz 2008, 33rd International Conference*(2008), pp. 1–2.
29. Y. Sun, B. M. Fischer, and E. Pickwell-MacPherson, "Effects of formalin fixing on the terahertz properties of biological tissues," J. Biomed. Opt. **14**(6), 064017 (2009).
30. L. L. K. Fu, N. Maffulli, K. M. H. Yip, and K. M. Chan, "Articular cartilage lesions of the knee following immobilisation or destabilisation for 6 or 12 weeks in rabbits," Clin. Rheumatol. **17**(3), 227–233 (1998).
31. L. L. K. Fu, N. Maffulli, and K. M. Chan, "Intra-articular hyaluronic acid following knee immobilisation for 6 weeks in rabbits," Clin. Rheumatol. **20**(2), 98–103 (2001).
32. E. Pickwell, B. E. Cole, A. J. Fitzgerald, M. Pepper, and V. P. Wallace, "In vivo study of human skin using pulsed terahertz radiation," Phys. Med. Biol. **49**(9), 1595–1607 (2004).
33. R. M. Woodward, B. E. Cole, V. P. Wallace, R. J. Pye, D. D. Arnone, E. H. Linfield, and M. Pepper, "Terahertz pulse imaging in reflection geometry of human skin cancer and skin tissue," Phys. Med. Biol. **47**(21), 3853–3863 (2002).
34. W. C. Kan, W. S. Lee, W. H. Cheung and E. Macpherson, "Terahertz Pulsed Imaging of Osteoarthritis," in BSN workshop (2008).

1. Introduction

The hallmark of osteoarthritis (OA) is the breakdown of cartilage and it usually affects the hands, feet and weight-bearing joints, such as knees, hips and spine. At worst, the cartilage cushion may completely wear away such that bones rub against each other causing inflammation, swelling and pain. Hyaline cartilage covers the subchondral bone to form the smooth articular surface of joints [1]. Hyaline cartilage can be further divided into three zones according to its regional organization. During the growth of the bone tissue, mineralization progressively takes place at the junction of hyaline cartilage and subchondral bone resulting in a layer of calcified cartilage with a tidemark separation. To illustrate the general cartilage structure and OA features histology of a femoral condyle with OA symptoms is given in Fig. 1. The cartilage is thinner and deteriorates in the region with OA. Poole's study provides further details on composition and structure of articular cartilage [2].

#132311 - $15.00 USD Received 26 Jul 2010; revised 16 Sep 2010; accepted 17 Sep 2010; published 20 Sep 2010

The prevalence of OA increases with age such that 1 in 5 adults aged 50-59 [3] and 9.6% of men and 18% of women aged over 60 have symptomatic osteoarthritis [4]. Therefore, it is a contemporary major medical challenge with high socioeconomic impact as early diagnosis and treatment of OA can help to prevent deterioration before irreversible damage is done. Current imaging diagnostic tools for OA are X-ray and MRI (magnetic resonance imaging), however, both of them are not able to detect early deterioration of cartilage. Therefore, there is a pressing need to develop a technique for detecting and monitoring changes in cartilage. This is particularly important in OA research where animal models are used as histology is currently the only technique to confirm the establishment and grade the severity of osteoarthritis [5] and requires sacrifice of many animals at different time points. A non-invasive imaging technique can help standardize the quantification of osteoarthritic grading and greatly reduce the number of animals sacrificed.

Previously, researchers have demonstrated the use of optical coherence tomography (OCT) for assessment the cartilage thickness and the result is quite promising in both *in vitro* [6] and *in vivo* cases [7]. Structural changes including surface erosion [8], hypocellularity [9], subsurface tears [10] were observed using OCT. In addition, OCT demonstrates the potential to detect changes at the early reversible stage of OA [11], through the loss of birefringence or birefringence changes in cartilage [9,12]. However, the image data can be difficult to interpret and prevents quantitative mapping of cartilage structure [13,14]. This has initiated our investigation to find other techniques to fill this gap. Here we have studied whether Terahertz pulsed imaging (TPI) has the ability to quantify OA or be an auxiliary method to compliment details seen in OCT images.

Several potential applications of THz to medicine have been investigated including skin cancer [15], breast cancer [16] and dentistry [17]. THz radiation possesses numerous characteristics that make it well suited for biomedical applications. For example, it is non-ionizing which means it would be safe to use for screening as well as diagnostic purposes. Through its sensitivity to molecular structures of biomolecules it can distinguish between: tissues [18], different chemicals within drugs [19], DNA bases [20] and polymorphic forms of medicines [21]. Thus, several research groups are focusing their efforts to developing waveguides to channel the THz beam to the sample [22,23]. Recently, a miniaturized THz endoscope system was developed by Ji *et al* [24] and it demonstrates the possibility of performing THz imaging inside the body thus opening up the future possibility of *in vivo* monitoring of osteoarthritis.

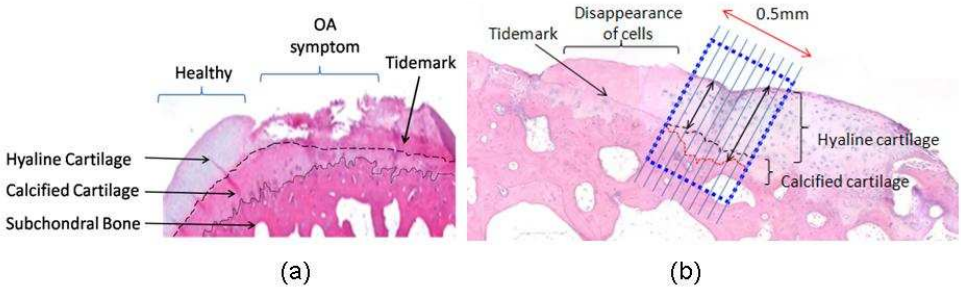

Fig. 1. (a) Histology of a femoral condyle with pronounced OA symptoms and (b) The dashed blue box indicates the measured region and the cartilage layer thicknesses of interest.

Cartilage thickness is a crucial measurement when diagnosing OA. Early experiments imaging cartilage with THz radiation were conducted by Knobloch *et al* [25] on excised pig larynx tissue. They demonstrated the absorption difference of THz radiation on the cartilage from the surrounding soft tissue. Subsequently, Jung *et al* [26] measured the THz spectral properties of human articular cartilage and showed differences between osteoarthritic cartilage and normal cartilage. Here we explored the potential of TPI to quantitatively measure

#132311 - $15.00 USD Received 26 Jul 2010; revised 16 Sep 2010; accepted 17 Sep 2010; published 20 Sep 2010

cartilage thickness building on a previous study [27,28] and extending our findings with additional measurements performed on formalin fixed rabbit femoral condyles with OA. Formalin fixing reduces the absorption of the tissue (by removing water which strongly absorbs THz radiation) [29]. Considering the effects of absorption independently, to see to the same depth in the fresh tissue the SNR for the measurement would need to be increased: $SNR_{Fresh} = (SNR_{Fixed})^{\alpha\_fresh/\alpha\_fixed}$, where α_fresh and α_fixed represent the absorption coefficients of the fresh and fixed tissue respectively. In this paper we have not made these measurements and they will be the subject of a follow up study. Advancements in terahertz technology are targeting increases in SNR as well as miniaturization to make intra-operative *in vivo* measurements possible in the future.

2. Experimental Methods

2.1 Sample preparation

Ethical approval was obtained from the Animal Experimentation Ethics Committee, Chinese University of Hong Kong, to harvest femoral condyle samples from twelve white New Zealand rabbits, aged 27-32 weeks. One leg of each rabbit had been immobilized by an aluminium splint for 6 weeks prior to harvesting. This protocol established OA symptoms in the immobilised leg and also potentially in other legs as the overall mobility of the rabbit was reduced. This protocol thus resulted in a variety of cartilage thicknesses [30,31]. All 24 samples were formalin fixed after excision and after the THz measurements, standard histology was performed. From the histology, as indicated in Fig. 2 for a typical sample, there is some variation in cartilage thickness within a sample. Thus when performing the measurements, we noted the location of the measurement to correlate with the thickness of the cartilage as determined from histology. We then calculated the mean and standard deviation of the cartilage layers from the histology by considering 10 points within the region of interest, as indicated within the dashed box in Fig. 1(b).

2.2 Imaging system

The system used for this study was a TPI™ Imaga1000 (TeraView Ltd., Cambridge, UK) the details of can be found setup can be found in Pickwell et al [32]. Data processing is often necessary to remove the system variability and extract the sample impulse function and was performed using the technique described by Woodward et al [33]. A double Gaussian band-pass filter is applied to remove both the low and high frequency noise components. The Gaussian filter function was selected carefully so that the OA features could still be resolved – if too many of the high frequency components were filtered out then the reflections from within the sample could not be resolved.

3. Results and discussion

3.1 Optical delays between reflections

In this work, we have measured and analyzed 12 pairs of samples (two samples from different legs of each rabbit). Typical THz impulse functions are shown in Figs. 2(a) and 2(b).

#132311 - $15.00 USD Received 26 Jul 2010; revised 16 Sep 2010; accepted 17 Sep 2010; published 20 Sep 2010

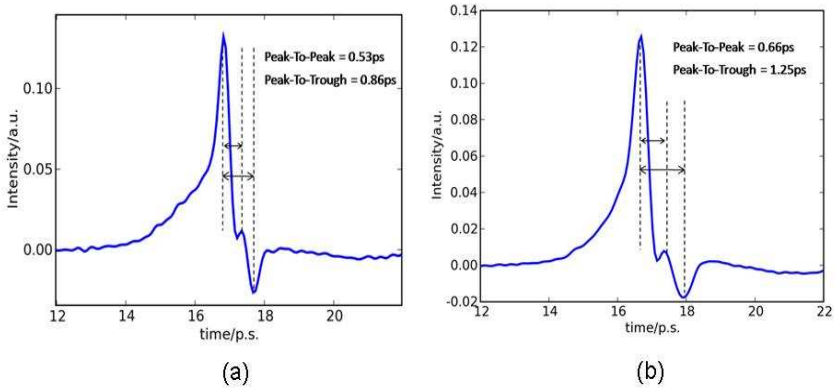

Fig. 2. The processed data from a pixel in the image of a typical (a) left sample and (b) right sample.

The first peak in the typical waveform represents the reflection from the quartz/sample interface. Those peaks or troughs after the first peak are reflections inside the sample caused by changes in refractive index between the hyaline and calcified cartilage layers. In Fig. 2(a), the optical delay between the first peak and second peak is 0.53ps and the optical delay between the first peak and trough is 0.86 ps. Both optical delays in the left sample are shorter than those in the corresponding right sample (0.66 ps and 1.25 ps respectively), which could be due to the left leg being immobilized for this animal.

Depth information of the femoral condyle helps to investigate the development of OA at the affected part. In Fig. 3 we demonstrate the cross-section view of a right leg sample in order to reveal the sample internal structure; the color gradient represents the amplitude of the processed impulse function. The green line indicates the position of quartz window and the black band is surface of the femoral condyle. A dark band indicated by the arrow above the bold black band is the result of the troughs of impulse functions (inset). This is the location of the hyaline/calcified cartilage interface.

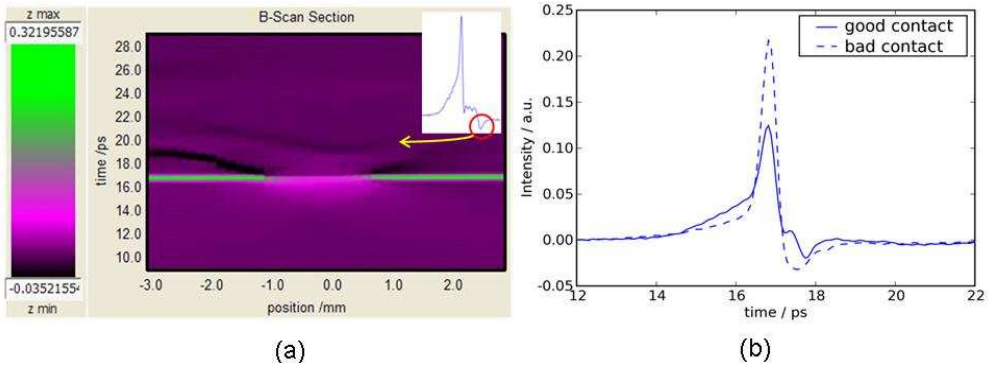

Fig. 3. (a) B-scan of a right sample (IM86R), a cross-section view with y-axis showing the depth profile. The arrow points to the interface formed by the reflected trough. So the space between two dark lines indicates the hyaline thickness if the trough is reflected off the cartilage/calcified cartilage interface. (b) It is important that the sample makes good contact with the quartz window. This graph illustrates how the waveforms for a sample are affected by the sample contact made with the quartz window.

Assuming the hyaline cartilage is homogeneous the reflections observed are most likely to have been caused by the hyaline cartilage/calcified cartilage interface and the cartilage/subchondral bone interface. The optical delay between reflections therefore indicates the thickness of the cartilage. When cartilage deteriorates due to OA, both the hyaline

#132311 - $15.00 USD Received 26 Jul 2010; revised 16 Sep 2010; accepted 17 Sep 2010; published 20 Sep 2010

cartilage and calcified cartilage can get thinner [28]. The shorter optical delays (both peak-to-peak and peak-to-trough) found in OA samples further support this hypothesis.

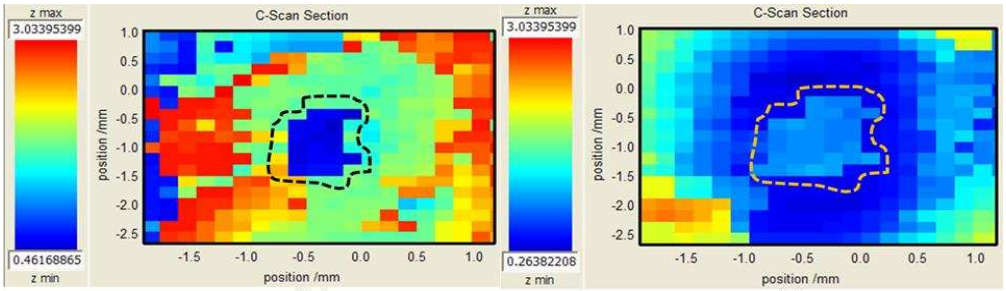

Fig. 4. Color map of a left sample (IM88L) with contrast representing the (a) peak-to-peak optical delay. The darker the blue represents a shorter peak-to-peak optical delay; and (b) the peak-to-trough optical delay.

The peak-to-peak and peak-to-trough optical delays of each pixel within the area of interest for all samples were calculated and plotted on false color maps an example is given in Fig. 4. Figure 4(a) shows the color map of peak-to-peak optical delays extracted from the sample and Fig. 4(b) shows the color map of its peak-to-trough optical delays. The process of how we constructed the peak-to-peak color map is illustrated in Kan *et al* [34]. In Fig. 4(a) only the center part in blue represents typical waveforms, in which the darker blue means the shorter the peak-to-peak optical delay is and the value under the color bar means the shortest peak-to-peak optical delay found in that image. In this case, it is about 0.46ps. It is very difficult to measure the refractive index (and absorption coefficient) of cartilage as the tissue properties vary with depth (and frequency); thus it is non-trivial to convert the optical delay into a distance. Therefore, in this study we have only looked for correlations between the optical delay and histology results.

Due to the sample geometry, not all the points made good contact with the quartz window. Generally, the area with good contact was less than $1mm^2$. Hence, typical waveforms appear only inside the darker blue region bounded by the dashed line in Fig. 4(a) where good contact was made. We determine whether or not a point has made good contact by assessing its peak value and the time flight of the first peak. Points with bad contact tend to have a much larger first peak value and the arrival time of the peak often lags behind those points in good contact. These differences are illustrated in Fig. 3(b) where a waveform from a pixel outside the dark blue region in the Fig. 4(a) (dashed line) is plotted alongside a waveform from within the dark blue region (solid line is). The lower peak value of the solid waveform verifies that the pixel is in good contact. Fifteen points were chosen in each sample from the area identified as having good contact and typically had waveforms like the one shown in inset Fig. 3(a). The mean and standard deviation of the optical delays were then calculated from these points. For comparison we took the average of total cartilage thickness (due to the hyaline and calcified layers) within the region of interest on the histology and compared to the mean optical delays. Data from 14 samples were rejected because there was too much variation in thickness within the region of interest.

#132311 - $15.00 USD Received 26 Jul 2010; revised 16 Sep 2010; accepted 17 Sep 2010; published 20 Sep 2010

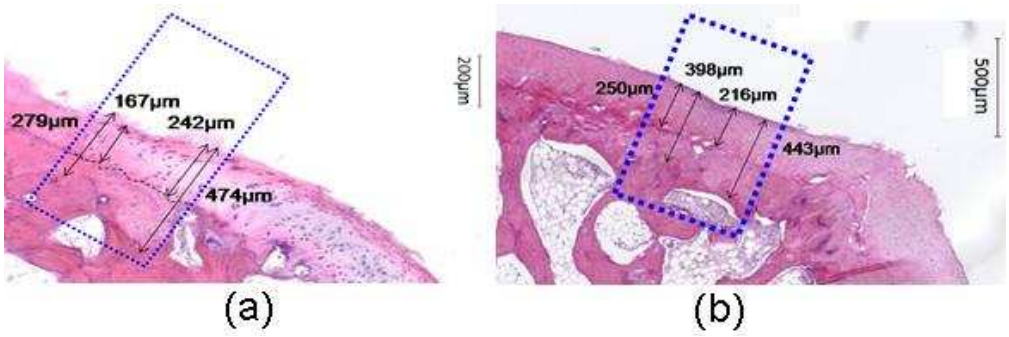

Fig. 5. The histology from animal 2 (IM86) of the (a) left sample and (b) right sample. The total cartilage thickness varies much more in the left sample (279-474 µm) compared to the right sample (398-443 µm).

For example, in Fig. 5 two histological slices from the right and left leg of the same animal are illustrated. The 0.5 mm wide dashed rectangle indicates the approximate location of the region of interest in Fig. 5. For the left sample [Fig. 5(a)] from the surface to the cartilage/bone interface, the thickness ranged from 279 µm to 474 µm. This high variation means that the cartilage had deteriorated too much in places for a meaningful correlation with the THz measurement to be determined and so this sample was not included in determining the relationship between the optical delay and cartilage thickness. However, as is clear from Fig. 5(b), the variation in the right sample was much less and so this sample was included.

The mean peak-to-trough optical delay values of the ten acceptable samples are plotted against their corresponding mean total cartilage thickness values from histology in Fig. 6. The correlation between the two measurements is 0.81. If we were to change the criterion on the histology requiring slightly less variation (such that sample 88L would be excluded), the correlation coefficient would increase to 0.87. This indicates that the natural variation within a sample combined with restricted image registration was a main limitation in this study.

3.2. Limitations due to formalin fixing

Formalin fixing had to be performed before the THz measurements because the samples were also being used for another study. This was not ideal as, in addition to making the samples rigid so that it was more difficult to place them on the quartz imaging window with good contact, the fixation process also affects the THz properties of the tissues [29], and can cause tissue shrinkage. The fixation process will have therefore made it more difficult for our THz measurements to determine and correlate the reflections between cartilage layers. Since we have seen promising results with the formalin fixed samples despite these limitations, this study provides motivation for further investigations using fresh tissue samples.

#132311 - $15.00 USD Received 26 Jul 2010; revised 16 Sep 2010; accepted 17 Sep 2010; published 20 Sep 2010

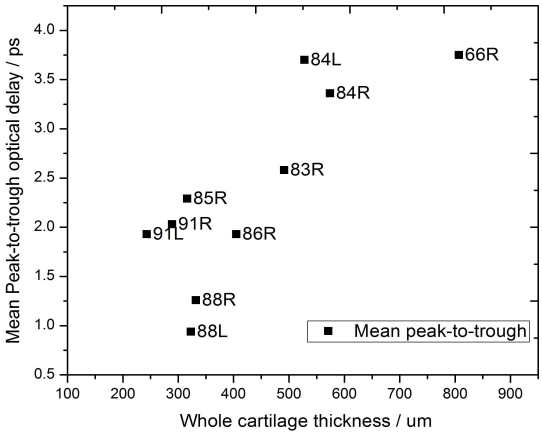

Fig. 6. A graph of the mean peak-to-trough THz optical delay against the mean total cartilage thickness from histology.

4. Conclusions

We have analysed the THz responses of cartilage from rabbit femoral condyle samples and found, by comparison with histology, that the reflected THz signal is sensitive to changes in the cartilage within a knee joint. The main limitation in this study was the restricted image registration of the THz system – it was not possible to match the location measured to histology beyond the nearest 0.5 mm. This, compounded with the large thickness variation within some samples meant that we can only draw limited conclusions. However, given that the correlation between the THz optical delay and the histology thickness for those valid samples was good ($r = 0.81$), this study indicates that further investigation would be worthwhile after THz imaging system improvements have been made. These early findings suggest that TPI has the potential to measure cartilage thickness once the THz properties of the constituent layers of cartilage have been better determined. It would be beneficial if we could develop TPI to use *in vivo* to monitor the development and treatment of OA in animal research models. Thus, TPI could improve the study of early stage OA and reduce the number of animals sacrificed by allowing the measurement the same animal multiple times.

Acknowledgments

The authors gratefully acknowledge partial financial support for this work from the Research Grants Council of the Hong Kong Government and the Shun Hing Institute of Advanced Engineering, Hong Kong.

#132311 - $15.00 USD Received 26 Jul 2010; revised 16 Sep 2010; accepted 17 Sep 2010; published 20 Sep 2010